New Journal of Physics
The open-access journal for physics

Background studies and shielding effects for the TPC detector of the CAST experiment

G Luzón[1], B Beltrán[2], J M Carmona, S Cebrián, H Gómez, I G Irastorza, J Morales, A Ortíz, A Rodríguez, J Ruz and J A Villar

Instituto de Física Nuclear y Altas Energías, Universidad de Zaragoza, Zaragoza, Spain
E-mail: luzon@unizar.es

New Journal of Physics **9** (2007) 208
Received 29 March 2007
Published 4 July 2007
Online at http://www.njp.org/
doi:10.1088/1367-2630/9/7/208

Abstract. Sunset solar axions traversing the intense magnetic field of the CERN Axion Solar Telescope (CAST) experiment may be detected in a time projection chamber (TPC) detector, as point-like x-rays signals. These signals could be masked, however, by the inhomogeneous background of materials in the experimental site. A detailed analysis, based on the detector characteristics, the background radiation at the CAST site, simulations and experimental results, has allowed us to design a shielding which reduces the background level by a factor of ∼4 compared to the detector without shielding, depending on its position, in the energy range between 1 and 10 keV. Moreover, this shielding has improved the homogeneity of background measured by the TPC.

[1] Author to whom any correspondence should be addressed.
[2] Present address: Department of Physics, Queens University, Kingston, ON, Canada.

PII: S1367-2630(07)47250-0

Contents

1. Introduction

The CERN Axion Solar Telescope (CAST) experiment [1] is placed at CERN and makes use of a decommissioned Large Hadron Collider (LHC) test magnet to look for solar axions through its Primakoff conversion into photons inside the magnetic field. The 10 m length magnet is installed on a platform which allows it to move $\pm 8^\circ$ vertically and $\pm 100^\circ$ horizontally to track the sun during sunset and sunrise. The 9 T magnetic field is confined in two parallel pipes of 4.2 cm diameter. At the end of the pipes, three detectors look for the x-rays originated by the conversion of the axions inside the magnet when it points to the sun. The two apertures of one of the ends of the magnet are covered by a conventional time projection chamber (TPC) [2] facing 'sunset' axions while in the opposite end, a charge coupled device (CCD) [3] coupled to an x-ray focusing telescope [4], and a Micromegas detector [5] search for 'sunrise' axions. The first results from the 2003 data analysis implied an upper limit to the axion–photon coupling $g_{a\gamma} < 1.16 \times 10^{-10}\,\mathrm{GeV}^{-1}$ [6]. A second set of measurements corresponding to 2004 with improved detectors and longer exposure set an upper limit on the axion–photon coupling of $g_{a\gamma} < 8.8 \times 10^{-11}\,\mathrm{GeV}^{-1}$ at 95% CL for axion masses $\leqslant 0.02$ eV [7].

All three detectors use discrimination techniques to reduce background contamination of the expected signal. The x-ray signal produced by the axions inside the magnet has a maximum at 4 keV and vanishes at around 10 keV [7]. More energetic deposits of energy, or signals outside the detector volume facing the apertures of the magnet, should be rejected. Simple requirements, depending on each detector, eliminate most of the background due to charged particles like cosmic rays, α and β radiation [2]–[5].

After the use of software cuts, the main source of background is expected to be γ rays produced predominantly in the radioactive chains of ^{238}U, ^{232}Th and in the ^{40}K isotope decays. Their interactions with material near the detectors can generate low energy photons via the Compton effect and also x-rays (such as those from copper identified in experimental spectra [3]). Additional sources are neutrons produced by fission and (α, n) processes or those induced by muons and cosmic rays. As the detector is moving tracking the sun, the background, and its

inhomogeneity, is a source of uncertainty since the axion signal is computed as the tracking (magnet pointing to the sun) minus the background (any other magnet orientation) signal. Therefore, not only low background levels but also a certain independence of the position are desirable to reduce uncertainties. The shielding presented here has been built for the TPC with this aim. In this article we will study the effects of the complete shielding installed in 2004, comparing its performance to the copper box used as shielding during the 2003 data taking period. For these studies, the energy range 3–7 keV has been chosen as the control region to analyse in order to be sure to eliminate threshold or saturation effects. Preliminary results were presented in [8].

In the first section, we will describe briefly the detector and the shielding. Next, the experimental site and its background will be analysed in detail taking into account γ and neutron sources. Monte Carlo simulations of the different sources of background will be discussed in section 4. In section 5, the effects of the shielding on background data will be studied. Finally, a few remarks summarizing the study.

2. The shielding of the CAST TPC detector

The CAST TPC detector has a conversion volume of $10 \times 15 \times 30\,\mathrm{cm}^3$ filled with Ar(95%)–CH_4(5%) gas at atmospheric pressure. The 10 cm drift direction is parallel to the magnet beam axis and perpendicular to the section of $15 \times 30\,\mathrm{cm}^2$ covering both magnet apertures. Two 6 cm diameter windows, consisting of very thin mylar foils (3 or 5 μm) stretched on a metallic strongback, allow the x-rays coming from the magnet to enter the chamber [2]. Except for the electrodes, the screws, the printed circuit board (PCB) and the windows, the entire chamber is made of 1.7 cm thick low radioactivity plexiglass.

A shielding around the TPC was designed to reduce the background in a complementary way to the effect of the off-line software cuts [2]. The requirements were to get a certain reduction of the background levels coming from external sources and a decrease of the background spatial inhomogeneity observed in the experimental site. The final design has been the result of a compromise between the shielding effect and technical limitations such as weight and size restrictions imposed by the experimental moving structure.

From inside to outside, the CAST TPC shielding (see figure 1) is composed of the following.

1. A copper box, 5 mm thick. This Faraday cage reduces the electronic noise and stops low energy x-rays produced in the outer part of the shielding by environmental γ radiation. It is also used for mechanical support purposes.
2. Lead bricks, 2.5 cm thick, which reduce the low and medium energy environmental γ radiation.
3. A cadmium layer, 1 mm thick, to absorb the thermal neutrons slowed down by the outer polyethylene wall.
4. Polyethylene pieces, 22.5 cm thick, used to slow the medium energy environmental neutrons down to thermal energies. It also reduces the γ contamination and helps the mechanical stability of the whole structure.
5. A PVC bag which covers the whole shielding assembly. This tightly closes the entire set-up allowing us to flush the inner part with pure N_2 gas coming from liquid nitrogen evaporation in order to purge this space of radon.

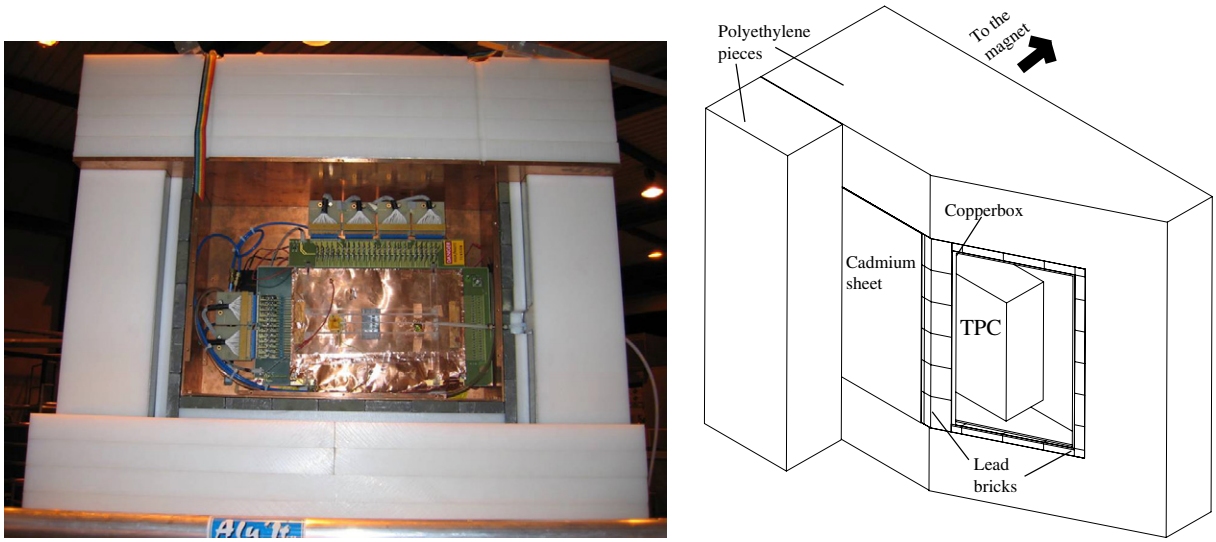

Figure 1. Picture on the left: TPC chamber inside the open shielding, consisting of: a copper box and lead, cadmium and polyethylene shields. A scheme has been drawn on the right to show the 3D arrangement of the whole structure.

6. A scintillating veto, $80 \times 40 \times 5\,\mathrm{cm}^3$, placed at the top of the shielding to reject muon-induced events working in anti-coincidence with the detector.

The described scheme is the outcome of several simulations and experimental tests. During the 2003 data taking period, the detector set-up consisted just of a copper box with N_2 gas flush. The full shielding was installed in 2004, after a test carried out in the real experimental conditions.

3. Experimental site and background

The CAST experiment in located in one of the buildings of the SR8 experimental area at CERN. The lower part of the walls around the apparatus is made of concrete. The materials for the upper part are, however, quite different: plastic in the north and concrete for the east and south walls with 11 cm thick metal pillars distributed every approximately 2.5 m all around. The north and east walls faced by the TPC detector during magnet movement are shown in figure 2.

The inhomogeneity of the building materials led us to undertake a careful study of the radioactive background and a detailed analysis of the measured TPC background data.

3.1. Gamma background

A hyper pure germanium γ spectrometer system, *in-situ* object counting system (ISOCS), based on a HpGe coaxial detector from Canberra has been used for γ ray measurements in a range from 50 keV to 3 MeV [9]. The γ spectrometry measurements confirmed the radioactive chains and potassium as the main sources for background and showed a background disparity between the different types of walls (see table 1).

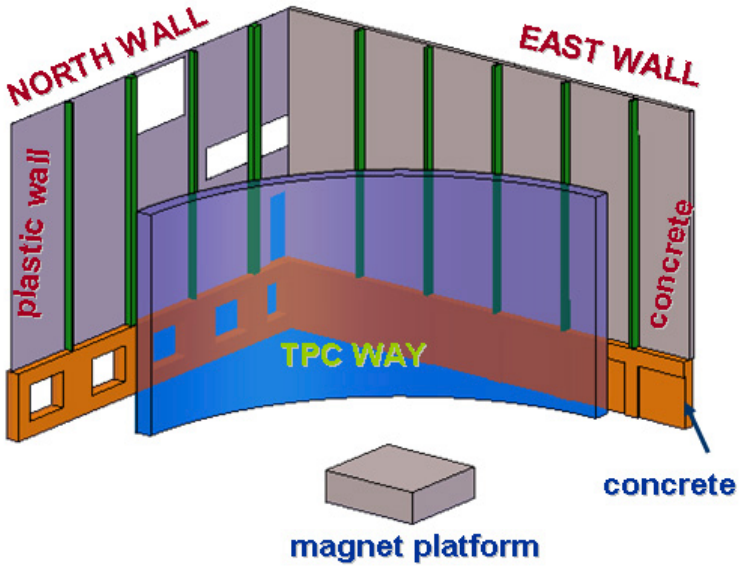

Figure 2. Graph shows the TPC detector path facing the north and east walls.

Table 1. Mean γ production in the CAST site (Bq kg^{-1}). For the radioactive chains, equilibrium activities are quoted. In the case of radon emanation from the ^{238}U chain, equilibrium is broken and activities for the nuclides before and after ^{222}Rn are given separately.

	^{238}U chain				
Wall description	^{238}U $\rightarrow^{226}$ Ra	^{218}Po $\rightarrow^{210}$ Po	^{235}U chain	^{232}Th chain	^{40}K
East (lower) and north pillars	25 ± 2		1.1 ± 0.7	10 ± 2	113 ± 10
East (upper) and south (upper)	923 ± 274	32 ± 5	40 ± 12	34 ± 6	388 ± 45

Assuming a concrete density around 2.4 g cm^{-3} and a wall thickness of 30 cm, we estimate the γ production in the lower part of every wall as $\sim$2.25 photons cm^{-2} s^{-1}, around 8 photons cm^{-2} s^{-1} in the upper part of the east and south walls and $\sim$2 photons cm^{-2} s^{-1} in the north wall pillars. We should also add around 6 photons cm^{-2} s^{-1} coming from the soil.

These data pointed also to a radon emanation for the east and south walls. Later radon measurements [9] gave mean values of 20 ± 10 Bq m^{-3} in summer and 15 ± 5 Bq m^{-3} in winter, not incompatible with a certain dependence on temperature.

Within this category, we could also include gammas arriving from radioactive contamination in the magnet platform, electronics material and also the contribution of the detector itself. Most of these materials are steel, plastics and metals (i.e. Fe, C, H, Cu, ...) whose impurities are also uranium, thorium and potassium.

Neutrons and protons coming from cosmic rays can also induce radioisotopes in the detector gas and materials (mainly ^{14}C and ^{3}H) whose contribution can be neglected owing to their low production rate (0.003 nuclei of ^{14}C and 0.001 nuclei of ^{3}H per litre per day in argon, computed considering saturation with a modified version of the COSMO [10] code based on the

semiempirical formulae of Silberberg and Tsao [11]). Another γ contribution corresponds to the cosmic ray photon flux, being only a small fraction ($\leqslant 1\%$) of the total [12].

Summarizing, the experimental site contributes to an important, and non-uniform, γ background owing to radioactive contamination. Most of the γ radiation described above would traverse the active volume of the detector without interacting at all due to the special features of the detector (only sensitive to energies of a few keV). However, energetic γ background loses part of its energy after interactions with materials surrounding the detector creating secondary photons which do contribute significantly to the background signal. Therefore, any shielding designed for the TPC detector should be a compromise between the external flux reduction and the increase of interactions in these materials as well as their own radioactive contamination. The best control of all these variables is achieved after Monte Carlo simulations plus experimental tests.

3.2. Neutron background

Even if the neutron component of the background is below the level of the typical γ background by three or four orders of magnitude, neutron signals in the detector could mimic those from x-rays.

Quantitative measurements of neutron background have been performed in the experimental site with a BF_3 detector. The homogeneous measured flux of neutrons in the CAST site is around $3 \times 10^{-2}\,\mathrm{cm}^{-2}\,\mathrm{s}^{-1}$. This value, and its homogeneity, points to a cosmic source. Cosmic ray generated neutrons have energies below a few GeV and the spectrum shows a dependence as $1/E^{0.88}$ up to 50 MeV and as $1/E$ above this energy [13]. This is the most important neutron contribution, not only for its intensity but also for its high energy. Other sources of neutron background are neutrons induced by muons in the surrounding materials, (α, n) reactions on light elements and spontaneous fission.

Muons interacting in shielding materials produce neutrons. FLUKA code [14] simulations with a measured total muon flux of $\sim 50 \times 10^{-3}\,\mathrm{cm}^{-2}\,\mathrm{s}^{-1}$ gave us a yield for neutrons entering the detector of $1.2 \times 10^{-3}\,\mathrm{cm}^{-2}\,\mathrm{s}^{-1}$ and a neutron spectrum peaking below 1 MeV. Most of these events are rejected by anti-coincidence with the veto installed as part of the shielding.

In nature mainly three nuclides (^{238}U, ^{235}U and ^{232}Th) undergo spontaneous fission. The rate of spontaneous fission of ^{238}U, the nuclide of shorter half life, is $0.218\,\mathrm{year}^{-1}\,\mathrm{g}^{-1}$ of concrete for 1 ppm of ^{238}U and the average number of neutrons emitted per fission event is 2.4 ± 0.2 with a typical evaporation spectrum peaking at around 1 MeV. Most of these fission neutrons will come from the concrete walls. Assuming a penetration for neutrons of 10 cm, we estimate the volume and surface production of neutrons in the concrete walls to be from around $0.60 \times 10^{-6}\,\mathrm{cm}^{-2}\,\mathrm{s}^{-1}$ for the lower east wall and $1 \times 10^{-6}\,\mathrm{cm}^{-2}\,\mathrm{s}^{-1}$ for the metal pillars to $30 \times 10^{-6}\,\mathrm{cm}^{-2}\,\mathrm{s}^{-1}$ in the upper east and south walls.

The α particles emitted in the radioactive chains can interact with other elements and produce neutrons through (α, n) reactions. For the upper south and east walls the final estimated neutron yield , following [15], is $\sim 10^{-5}\,\mathrm{cm}^{-2}\,\mathrm{s}^{-1}$. The radioactive activity of soil (or of the lower east wall) will produce one order of magnitude less of neutrons $\sim 10^{-6}\,\mathrm{cm}^{-2}\,\mathrm{s}^{-1}$. The energy spectra for these neutrons consist of peaks related to α particles energies, with 8.79 MeV being the highest energy for naturally emitted α particles (decay of ^{212}Po).

In summary, we have collected all the neutron productions in table 2. The energetic cosmic component appears to be the most relevant contribution.

Table 2. Comparison of the estimated order of magnitude for neutrons coming from different sources. Values are given in neutrons per cm^2 per second.

Cosmic	Muon induced	Fission	(α, n)
$\sim 10^{-2}$	$\sim 10^{-3}$	$\sim 10^{-5}$	$\sim 10^{-5}$

4. Monte Carlo simulations

A complete set of Monte Carlo simulations has been carried out in order to estimate the external background contribution to the TPC detector data during the 2003 and 2004 taking data periods. We have not only reproduced the TPC detector and its shielding in the simulations, but also the main software cuts to be able to discriminate the expected x-ray signal. They show that the use of cuts reduce the registered events by two orders of magnitude in good agreement with the experimental data. This fact results in low statistics, having to establish a compromise between computing time and non-negligible statistical errors. Despite this, Monte Carlo simulations have been very useful to understand and quantify the number of counts coming from the external background in the 2003 and 2004 sets of data of the TPC detector.

The background level (in the 3–7 keV region of interest) for three different shielding configurations have been compared: a 5 mm thick copper box, the copper box plus 2.5 cm of lead, and a complete shielding consisting of 5 mm thick copper box plus 2.5 cm of lead plus 22.5 cm of polyethylene.

First of all we will focus on γ simulations since this is the main contribution to the TPC background, then we will make a few comments about neutron simulations, though they are quite difficult to verify experimentally.

4.1. Simulations for external γ

These simulations have been performed using the GEANT4 code [16] since it allows to take into account all the aspects of the simulation process including the detector response. The primary events, corresponding to the radioactive chains and potassium, have been generated uniformly and isotropically on a sphere surrounding the most external surface of the shielding.

The shielding made of 5 mm of copper plus 2.5 cm of lead plus 22.5 cm of polyethylene reduces the external γ background by more than one order of magnitude, $(92\pm3)\%$ in the 3–7 keV range. Since the thick layer of polyethylene helps in the γ attenuation, the same shielding without polyethylene is about a 15% less effective, causing an estimated reduction of $(77\pm4)\%$. Compton interactions in the polyethylene result in lower energy photons which are easily absorbed in the lead. Though a thicker layer of lead could stop a larger fraction of the external γ's, it can be a source of secondary neutrons and it would add too much weight to one of the ends of the magnet.

Due to the spatial inhomogeneity of the γ background coming from walls, simulations allow us to make just a rough estimate of the TPC recorded counts. These external photons cause between 30 and 55 counts h^{-1} in the volume of the detector facing the two windows for the 3–7 keV energy region in the case of the copper shielding (2003 data), and between 2 and 5 counts h^{-1} in the case of the complete shielding configuration of 2004. This result, as we will see in the next section, is compatible with measured data.

The GEANT4 package has also been used to simulate the effect of the radon trapped inside the copper box. Radon decays have been produced isotropically in the volume between the TPC and the copper box. These simulations quantify the point-like signals in the 3–7 keV range as 0.04 counts h^{-1} for an overestimated radon concentration of 25 Bq m^{-3}. Therefore, the radon contribution to the background can be neglected in the 2003 and 2004 shielding conditions due to the plastic bag around the entire set-up and the nitrogen flush.

4.2. Neutron simulations

Though neutrons interacting in materials can produce γ particles, more neutrons, α particles and fission fragments depending on materials and energies, the most efficient reaction is the elastic scattering, energy transferred to nuclear recoils. This energy is determined by the energy of the incident neutron (E_n) and the scattering angle θ

$$E_R = \frac{4A}{(1+A)^2}(\cos^2\theta)E_n. \tag{1}$$

In the case of argon, $A = 40$, assuming a quenching factor of 0.28, the maximum visible energy and the neutron energy are related as follows

$$E_{Rmax} = 0.0266E_n. \tag{2}$$

Therefore, the neutrons able to deposit a visible energy in the analysed range of 3–7 keV are mostly those with an energy between 0.11 and 0.27 MeV.

A GEANT4 simulation, using G4NDL3.5 high precision neutron data library and a real cosmic spectrum as input, has been carried out. This simulation has allowed us to roughly estimate about 2 counts h^{-1} caused by cosmic neutrons inside the two windows of the TPC in the (3–7) keV visible energy region in the case of the copper shielding. As we will show in section 5, this rate is between 25–45 times smaller than the counting rates in 2003.

To understand the effects of the different layers of shielding we have used the FLUKA code of proven reliability for the transport of neutrons. This second simulation shows the effects of every layer of shielding material on cosmic neutrons: while polyethylene decreases the number of background neutrons per cosmic neutron, the 2.5 cm of lead increases this number (see figure 3) due to $(n, 2n)$ processes (observe the evaporation spectrum). Cadmium absorbs thermal and epithermal neutrons with energies below 1 keV.

The shielding without polyethylene has been also compared to the complete configuration. The number of cosmic neutrons able to produce nuclear recoils and a deposit of visible energy in the TPC in the 3–7 keV range decreases by only 20% after the complete shielding due to the production of neutrons in lead. The number of neutrons could even increase by 10% if the 22.5 cm of polyethylene are taken off. Then, the shielding hardly reduces the amount of neutrons and it would increase the number without polyethylene. This background contribution has been estimated at around 1.5 counts h^{-1} for the 2004 shielding conditions.

The neutron production in the shielding due to muons has also been investigated. Most of these neutrons are produced in lead. As mentioned in section 3.2, the number of neutrons produced by each sea level muon is 0.024, giving a neutron flux reaching the detector of 1.2×10^{-3} cm^{-2} s^{-1}, six orders of magnitude higher than that calculated in [17] for a thicker shielding but a much less intense underground muon flux. We can roughly estimate about 0.02 counts h^{-1} inside the

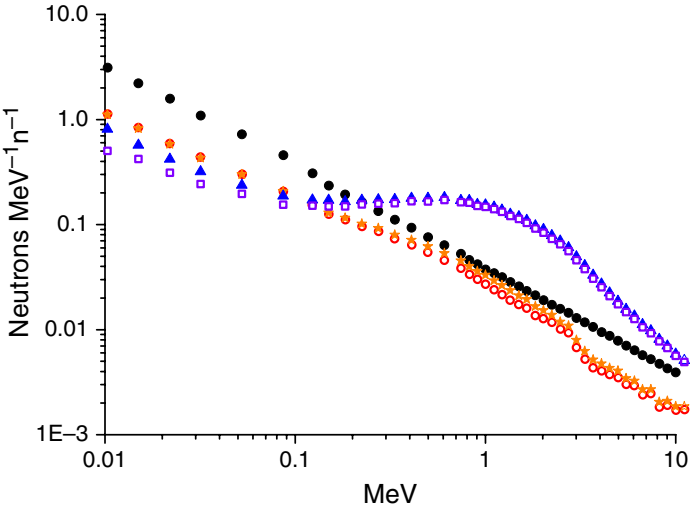

Figure 3. Cosmic neutrons in the 10 keV–20 MeV range after traversing every layer of shielding: incoming cosmic neutrons (solid circles), neutrons after traversing 22.5 cm of polyethylene (open circles) plus 1 mm of cadmium (solid stars) plus 2.5 cm of lead (solid triangles) plus 5 mm of copper (open squares). Spectra are normalized to one cosmic neutron.

windows corresponding to neutrons induced by muons, three orders of magnitude smaller than the measured background rates.

Regarding other population of neutrons, we have not considered those coming from radioactivity (fission and (α, n) processes) since 22.5 cm of moderator would reduce their tiny contribution (of the order of 10^{-5} cm^{-2} s^{-1}) by two orders of magnitude [17].

5. TPC background data

First tests of the full shielding (with a 5 cm thick layer of lead in this case) at the laboratory showed a reduction factor of ∼8 below the background level of the chamber, without any shielding or nitrogen flush, for energies between 1 and 10 keV. Once the detector was mounted in the magnet on the moving platform, this factor became ∼4.3 (∼6.4 in the 6–10 keV range).

After these first tests, another set was undertaken at the CAST experimental site to observe the effects of every component of the shielding. The magnet was placed in horizontal position facing the NE corner, far away from the forced air windows and in an intermediate position between the north and the east wall in order to get a more *average* flux. Here we measured the TPC background in different shielding conditions. For this position, it has been checked that the full shielding (copper plus lead plus polyethylene) reduces background levels by a factor of ∼3 in the 3–7 keV energy interval, in comparison to the copper shielding, thanks mainly to the 2.5 cm of lead, while a double layer of lead (5 cm) does not improve these results (see figure 4). When comparing the experimental reduction factor from those obtained in simulations, it must be kept in mind that in the latter we were just dealing with external γ radiation, forgetting about internal contamination or radon intrusion which contribute to measurements in all shielding conditions. Another reason for the discrepancies lies in the fact that in simulations the shielding

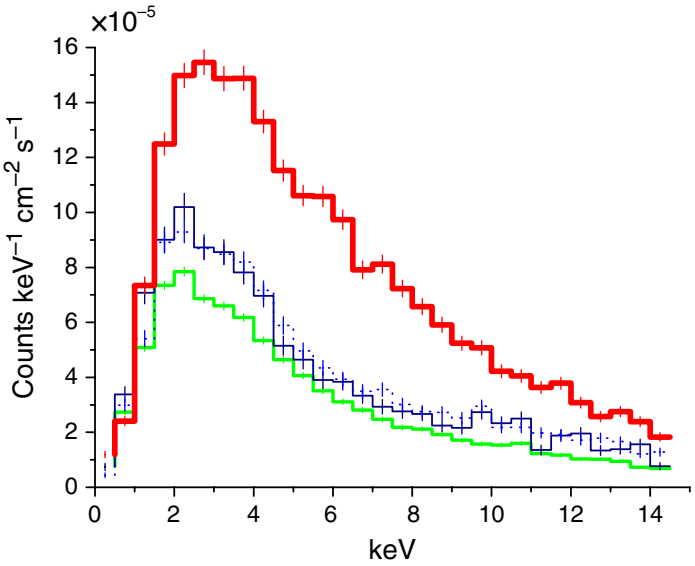

Figure 4. Background data obtained in the shielding test at the experimental site for different shielding configurations: full shielding set-up (bottom line), the copper box plus 2.5 cm of lead (solid line in the middle), the copper box plus a double layer of lead (dotted line in the middle) and just the copper box (upper line).

is all around the detector while the TPC is actually attached to the magnet pipes, and thus partially not shielded. As a consequence of these two reasons, the background level decrease is lower than expected after simulations.

Another experimental test was performed to quantify the contribution of the radon trapped in the copper box. Measurements were carried out with and without nitrogen flush at the same spatial position and one right after the other to avoid time variations. The subtracted spectrum (without and with nitrogen flush) can be thought of as due to the radon inside the copper box since the plastic bag prevents the outer radon from entering the shielding. Despite the poor statistics, the estimated radon rate in the 3–7 keV range for point-like signals (0.13 ± 2.33 counts h^{-1}) in the volume facing the two windows of the TPC, shows a negligible contribution to the background and is compatible with the 0.04 counts estimated in simulations.

Finally, we can also compare the experimental background data, since during the two data taking periods (years 2003 and 2004) the TPC detector has recorded not only tracking data, when the opposite part of the magnet is pointing to the sun, but also background data at any other time of the day. In order to get the best control of the background and determine its inhomogeneity, these measurements have been performed at precise horizontal (movement along a circle) and vertical positions. Figure 5 shows measured background levels for nine positions: the three first measurement points are facing the north wall; the three next points face the NE corner and the last one faces the east wall near one of the metal pillars. During the year 2003, with the TPC covered by a 5 mm thick copper box and a nitrogen flush inside, the background measurements showed a high degree of inhomogeneity as can be observed. Higher background rates are registered in the proximity of more intense sources of radioactivity such as the upper part of the east wall or the soil while the closeness to a metal pillar or to the plastic wall (upper part of north wall),

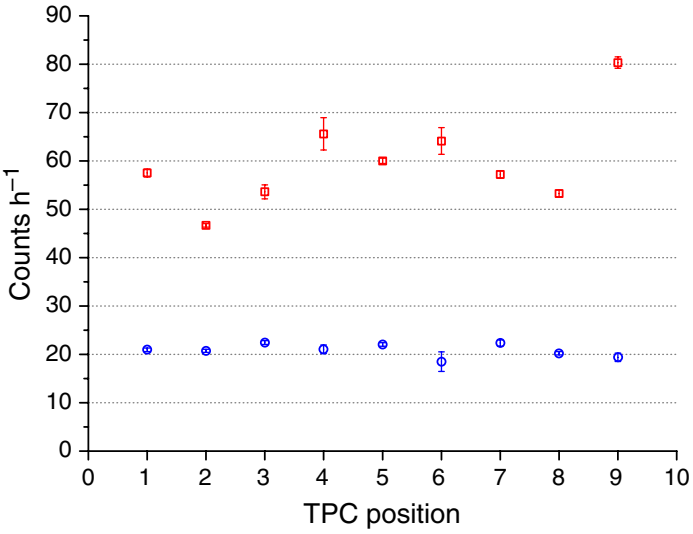

Figure 5. July–August background data for 2003 (squares) and 2004 (circles). Measurements correspond to three vertical positions and three horizontal positions of the TPC detector. The nine magnet positions run first vertically and then horizontally.

decreases rates. Also metal components such as scaffolding, ladders, . . . can affect measurements at some points. Thanks to the shielding described in section 2, the 2004 background data show rate reductions by more than a factor of 2.5, reaching even a factor of 4 at some positions (see figure 5). Moreover, the background is now fairly homogeneous.

When comparing these experimental data with the results of the simulations presented in the previous section, one notes that the background reduction obtained with the shielding is larger in the external γ simulations (a reduction factor of 10–15) than in the experimental data (2.5–4). This seems to imply that, while most of the background in the 2003 set-up was indeed linked to the external γ background (as proved by its inhomogeneity and the effectiveness of the shielding), most of the remaining background in the 2004 set-up must be of a different origin from those included in the simulations. The most probable candidates are internal contaminations of the components inside the shielding, or background coming from the side where the detector is attached to the magnet (and necessarily unshielded), from contaminations present for instance in the magnet components. This hypothesis fits well with the fact that this contribution is constant for every magnet position. As shown in table 3, where all calculated and measured background levels are collected, a speculated constant internal contamination (first column) of about 15 counts h^{-1} would fit the overall scenario. Whatever the precise origin of the remaining background, the effect of the shielding on the 2005 TPC operation, both in terms of reduction of background and its variability, yielded a substantial increase of sensitivity of the detector in the context of the CAST experiment [7], when compared to the previous 2003 period.

Table 3. Estimated external background contribution to TPC data corresponding to the years 2003 and 2004. Values are given in counts h^{-1} and correspond to estimated point-like, 3–7 keV energy, deposits in the TPC volume facing the two windows of the chamber, compared to the mean measured values.

	Monte Carlo estimates					
Year	Internal contamination	External γ sources	Cosmic neutrons	μ-induced neutrons	Radon	Measured values
2003	15	30–55	2		0.04	47–80
2004	15	2–5	1.5	0.02	0.04	19–21

6. Summary and conclusions

After a characterization of the radioactive contamination, we present herein the effects of a shielding on the CAST TPC detector background data. Requirements of a reduction of the background levels and of a decrease of the background inhomogeneity have been fulfilled.

γ measurements have reported a clear inhomogeneus radioactive contamination due to the uranium and thorium radioactive chains and to potassium and radon emanation from the east and south wall. Also neutrons have been studied, the cosmic neutrons being the most relevant contribution. Other background contaminants can be neglected.

Then, after the identification of the background sources, we have undertaken Monte Carlo simulations which have allowed us to understand the TPC detector response to γ and neutron sources as well as the effects of different components of shielding on the background levels. As a result of these simulations, we have learned that 2.5 cm of lead reduces the external γ background in the 3–7 keV range by $(77 \pm 4)\%$ but produces neutrons due to high-energy cosmic neutron and muon interactions. The addition of a 22.5 cm layer of polyethylene results in a $(92 \pm 3)\%$ reduction of the γ background, decreases by 20% the cosmic neutrons and eliminates any low energy neutrons. These results are compatible with experimental tests performed at the CAST site. For all these reasons the installed shielding in 2004 consists of 5 mm of copper plus 2.5 cm of lead plus 22.5 cm of polyethylene.

Finally, the 2004 data confirm a reduction of background levels by a factor of between 2.5 and 4 from the 2003 data (the highest for positions close to the most intense γ sources) as well as a quite acceptable degree of homogeneity. For this period, most of the contamination is due to sources near the detector (around 15 counts h^{-1} in the volume facing the two windows for the 3–7 keV energy interval), while external γ radiation and cosmic neutrons only add 3–6 counts h^{-1} to the TPC detector background for the same interval of energies.

Acknowledgments

This research was partially funded by the Spanish Ministerio de Educación y Ciencia (MEC) under contract FPA2004-00973 and promoted within the ILIAS (Integrated Large Infrastructures for Astroparticle Science) project funded by the EU under contract EU-RII3-CT-2003-506222. We thank the CAST Collaboration for their support. We are also grateful to the group of the Laboratorio Subterráneo de Canfranc (LSC) for material radiopurity measurements.

References

[1] Zioutas K *et al* 1999 *Nucl. Instrum. Methods* A **425** 480
[2] Autiero D *et al* 2007 *New J. Phys.* **9** 171(*Preprint* physics/0702189)
[3] Kuster M *et al* 2007 *New J. Phys.* **9** 169 (*Preprint* physics/0702188)
[4] Lutz G *et al* 2004 *Nucl. Instrum. Methods* A **518** 201
[5] Abbon P *et al* 2007 *New J. Phys.* **9** 170 (*Preprint* physics/0702190)
[6] Zioutas K *et al* (CAST Collaboration) 2005 *Phys. Rev. Lett.* **94** 121301
[7] Andriamonje S *et al* (CAST Collaboration) 2007 *J. Cosmol. Astropart. Phys.* JCAP04(2007)010 (*Preprint* hep-ex/0702007)
[8] Ruz J *et al* 2006 *Proc. 9th Int. Conf. on Topics in Astroparticle and Underground Physics 2005 (TAUP05) J. Phys.: Conf. Ser.* **39** 191
[9] CAST Technical paper in preparation
[10] Martoff C J *et al* 1992 *Comput. Phys. Commun.* **72** 96
[11] Silberberg R and Tsao C H 1973 *Astrophys. J. Suppl. Ser.* **25** 315
Silberberg R and Tsao C H 1973 *Astrophys. J. Suppl. Ser.* **25** 335
[12] Heusser G 1995 *Annu. Rev. Nucl. Part. Sci.* **45** 543
[13] Hess W N *et al* 1959 *Phys. Rev.* **116** 445
[14] Fassò A *et al* 2000 *Proc. Monte Carlo 2000 Conf. (Lisbon)* ed A Kling, F Barao, M Nakagawa, L Tavora and F Vaz (Berlin: Springer-Verlag) p 159
Fassò A *et al* 2001 *Proc. Monte Carlo 2000 Conf. (Lisbon)* ed A Kling, F Barao, M Nakagawa, L Tavora and F Vaz (Berlin: Springer-Verlag) p 955
[15] Wulandari H *et al* 2004 *Astropart. Phys.* **22** 313
[16] Agostinelli S *et al* (GEANT4 Collaboration) 2003 *Nucl. Instrum. Methods* A **506** 250
[17] Carmona J M *et al* 2004 *Astropart. Phys.* **21** 523